Supplementary Information for

Sequentially-Regular Polymer Acceptors Featuring Flexible Spacers for High-Performance and Mechanically-Robust All-Polymer Solar Cells

Jin-Woo Lee,[⊥,a] *Cheng Sun,*[⊥,b] *Sun-Woo Lee,*[c] *Geon-U Kim,*[a] *Sheng Li,*[a] *Cheng Wang,*[d] *Taek-Soo Kim,*[c] *Yun-Hi Kim*[*,b] *and Bumjoon J. Kim*[*,a]

[a] *Department of Chemical and Biomolecular Engineering, Korea Advanced Institute of Science and Technology (KAIST), Daejeon 34141, Republic of Korea*

[b] *Department of Chemistry and RIGET, Gyeongsang National University, Jinju 52828, Republic of Korea*

[c] *Department of Mechanical Engineering, KAIST, Daejeon 34141, Republic of Korea*

[d] *Advanced Light Source, Lawrence Berkeley National Laboratory, 1 Cyclotron Road, Berkeley, CA 94720, United States*

[*] *All correspondence should be addressed to B. J. K. and Y.-H. Kim (E-mail: bumjoonkim@kaist.ac.kr, ykim@gnu.ac.kr)*

Experimental Section

***Materials*:** 4,8-Bis(4-chloro-5-(2-ethylhexyl)thiophen-2-yl)-4,8-dihydrobenzo[1,2-b:4,5-b']dithiophene-2,6-diyl)bis(trimethylstannane) was purchased from the Solarmer materials inc. All the other eluents and materials were prepared from Sigma Aldrich Co. and Tokyo Chemical Industry Co. 1,8-Bis(5-(trimethylstannyl)thiophen-2-yl)octane, IC-Br-In, Y5-20-In, and PYBDT were synthesized according to previous reports.[1-5] 2,9-Bis(3-((3-(dimethylamino)propyl)amino)propyl)anthra[2,1,9-*def*:6,5,10-*d'e'f'*]diisoquinoline-1,3,8,10(2*H*,9*H*)-tetraone (PDINN) was synthesized by following the method described in the literature.[6] Poly[(9,9-bis(3′-((*N*,*N*-dimethyl)-*N*-ethylammonium)propyl)-2,7-fluorene)-*alt*-5,5′-bis(2,2′-thiophene)-2,6-naphthalene-1,4,5,8-tetracaboxylic-*N*,*N*′-di(2-ethylhexyl)imide]dibromide (PNDITF3N-Br) was synthesized according to the reported method.[7] Poly[(2,6-(4,8-bis(5-(2-ethylhexyl)thiophen-2-yl)benzo[1,2-b:4,5-b′]dithiophene)-co-(1,3-di(5-thiophene-2-yl)-5,7-bis(2-ethylhexyl)-benzo[1,2-c:4,5-c′]dithiophene-4,8-dione)] (PBDB-T) was purchased from Brilliant Matters Co.

Synthesis of polymer acceptors and their intermediates

(1) Synthesis of Y5-20-In

12,13-bis(2-octyldodecyl)-3,9-diundecyl-12,13-dihydro-[1,2,5]thiadiazolo[3,4-e]thieno[2",3":4',5']thieno[2',3':4,5]pyrrolo[3,2-g]thieno[2',3':4,5]thieno[3,2-b]indole-2,10-dicarbaldehyde (690 mg, 0.5 mmol) and IC-Br-In (560 mg, 2 mmol) were added into a mixture of chloroform (100 mL) and pyridine (5 mL). The mixture was stirred for overnight in an oil bath at 65 °C. After being cooled down to room temperature, the solvent was removed at reduced pressure (200 mbar). The residual product was purified by silica-gel packed column chromatography using dichloromethane/hexane as eluent to give Y5-20-In as a black solid (520 mg, 63%).

^{1}H NMR (300 MHz, CD_2Cl_2) δ 9.10 (s, 2H), 8.51 (d, J = 8.4 Hz, 2H), 8.03 (d, J = 1.9 Hz, 2H), 7.86 (dd, J = 8.4, 2.0 Hz, 2H), 4.84 (d, JZ = 7.8 Hz, 4H), 3.26 – 3.08 (m, 4H), 2.22 (s, 2H), 1.87 (t, J = 8.1 Hz, 4H), 1.50 (m, 4H), 1.41 – 0.74 (m, 110H).

^{13}C NMR (125 MHz, $CDCl_3$) δ 187.04, 159.98, 153.73, 147.61, 145.24, 138.63, 137.80, 136.09, 135.60, 134.31, 133.60, 130.91, 129.58, 126.83, 126.49, 120.22, 115.41, 115.05, 113.66, 68.45, 55.81, 39.32, 32.06, 32.00, 31.36, 30.73, 30.03, 29.95, 29.82, 29.78, 29.72, 29.68, 29.61, 29.57, 29.50, 29.38, 25.80, 22.84, 22.77, 14.27. NMR data match well with the previous report.[2, 5]

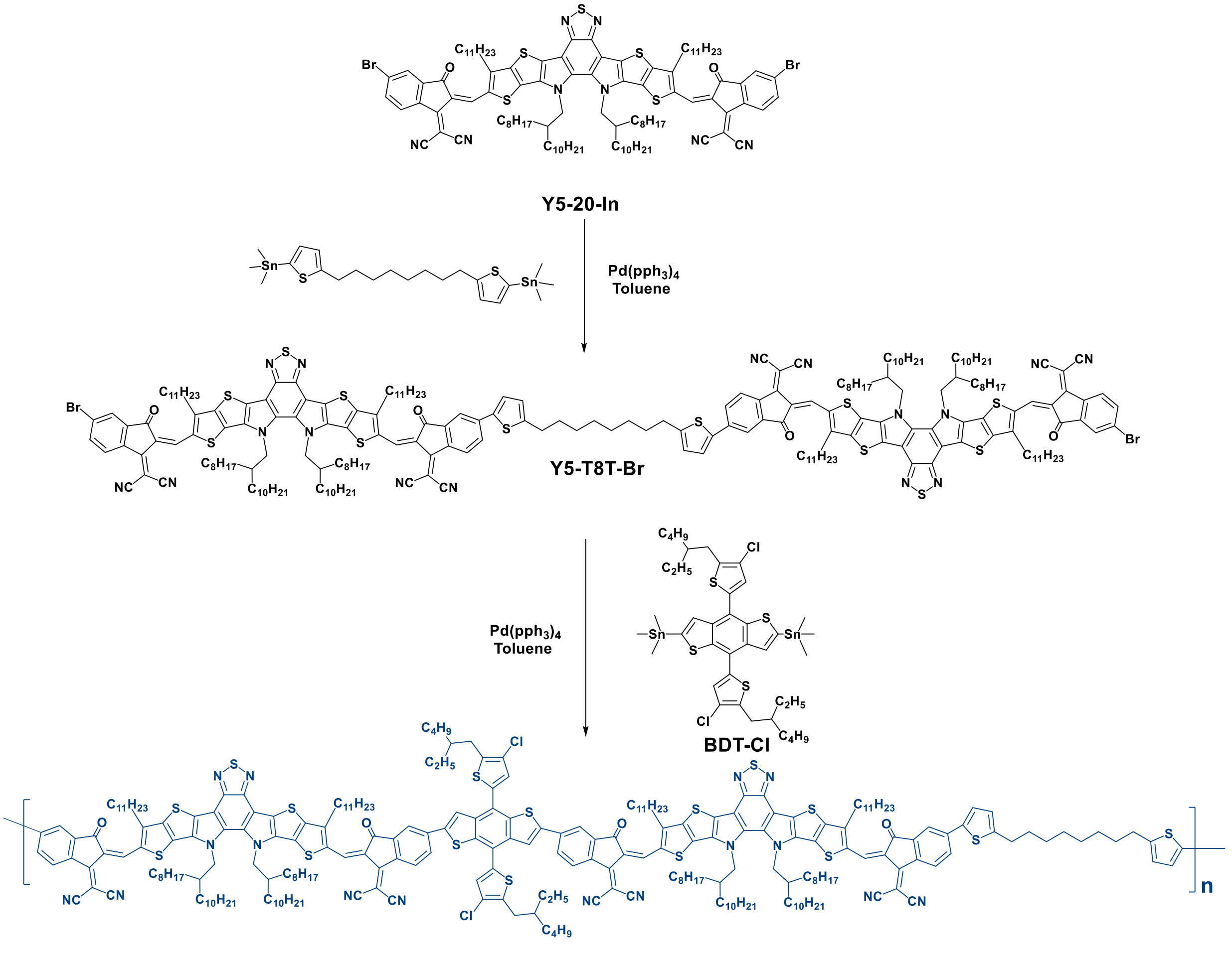

Scheme S1. Synthetic scheme for Y5-T8T-Br and PYFS-Reg.

(2) Synthesis of Y5-T8T-Br

Y5-20-In (500 mg, 0.267 mmol), 1,8-bis(5-(trimethylstannyl)thiophen-2-yl)octane (54 mg, 0.089 mmol), and Pd(pph$_3$)$_4$ (5 mg, 0.0044 mmol) were combined in a 100 mL two-necked flask (**Scheme S1**). Anhydrous toluene (40 mL) was added under the argon atmosphere. The mixture was reacted for 12 h at 110 °C. After being cooled down, the solvent was removed at reduced pressure (200 mbar). The residual product was purified by silica-gel packed column chromatography using chloroform/hexane as eluent to give Y5-T8T-Br as a black solid (330 mg, 33%).

^{1}H NMR (300 MHz, CDCl$_3$) δ 9.07 (d, J = 21.5 Hz, 4H), 8.52 (dd, J = 22.6, 8.4 Hz, 4H), 8.03 (dd, J = 7.8, 1.4 Hz, 4H), 7.78 (dd, J = 8.5, 1.6 Hz, 4H), 7.41 (d, J = 3.6 Hz, 2H), 6.87 (d, J = 3.4 Hz, 2H), 5.16 – 4.43 (m, 8H), 3.40 – 2.99 (m, 8H), 2.90 (t, J = 7.4 Hz, 4H), 2.22 (s, 4H), 1.91 – 1.72 (m, 12H), 1.54 – 0.69 (m, 236H). ^{13}C NMR (125 MHz, CDCl$_3$) δ 188.31, 186.97, 160.04, 159.83, 153.74, 152.80, 149.74, 147.62, 147.57, 145.15, 145.07, 140.72, 139.36, 138.60, 138.39, 138.08, 137.93, 137.90, 137.66, 137.60, 136.25, 135.49, 135.47, 135.27, 134.58, 134.44, 133.76, 133.52, 133.49, 130.94, 130.91, 130.06, 129.48, 126.77, 126.75, 126.39, 126.22, 126.07, 125.88, 121.44, 120.01, 118.81, 115.68, 115.43, 115.41, 115.06, 113.84, 113.44, 68.30, 67.32, 32.06, 32.01, 31.97, 31.62, 31.33, 31.23, 30.77, 30.61, 30.03, 30.00, 29.97, 29.83, 29.79, 29.77, 29.71, 29.70, 29.61, 29.58, 29.54, 29.50, 29.41, 29.25, 25.83, 22.83, 22.79, 14.26.

(3) Synthesis of PYFS-Reg

Y5-T8T-Br (250 mg, 0.065 mmol), 4,8-bis(4-chloro-5-(2-ethylhexyl)thiophen-2-yl)-4,8-dihydrobenzo[1,2-b:4,5-b']dithiophene-2,6-diyl)bis(trimethylstannane (63 mg, 0.065 mmol), and Pd(pph$_3$)$_4$ (3.8 mg, 0.0032 mmol) were combined in a 10 mL two-necked flask (**Scheme S1**).

Anhydrous toluene (6 mL) was added under the argon atmosphere. The mixture was reacted for 24 h at 110 °C. After being cooled down, the reactant mixture was poured into methanol. The precipitate was filtered and Soxhlet extracted with methanol, hexane, and chloroform sequentially. The extracted solution was concentrated and precipitated into 200 mL methanol, filtered and dried under vacuum to give the PYFS-Reg as a dark solid. (160 mg, 72%); (The number-average molecular weight (M_n)= 24 kg mol^{-1}, Dispersity (*Đ*)= 1.7).

^{1}H NMR (300 MHz, CDCl$_3$) δ 9.43 – 8.92 (broad, 2H), 8.92 – 8.47 (broad, 2H), 8.34 – 7.70 (broad, 5H), 7.60 – 7.33 (broad, 2H), 7.10 – 6.71 (broad, 1H), 5.30 – 4.36 (broad, 4H), 3.40 – 2.66 (broad, 8H), 2.43 – 2.08 (broad, 2H), 2.08 – 0.45 (broad, 139H).

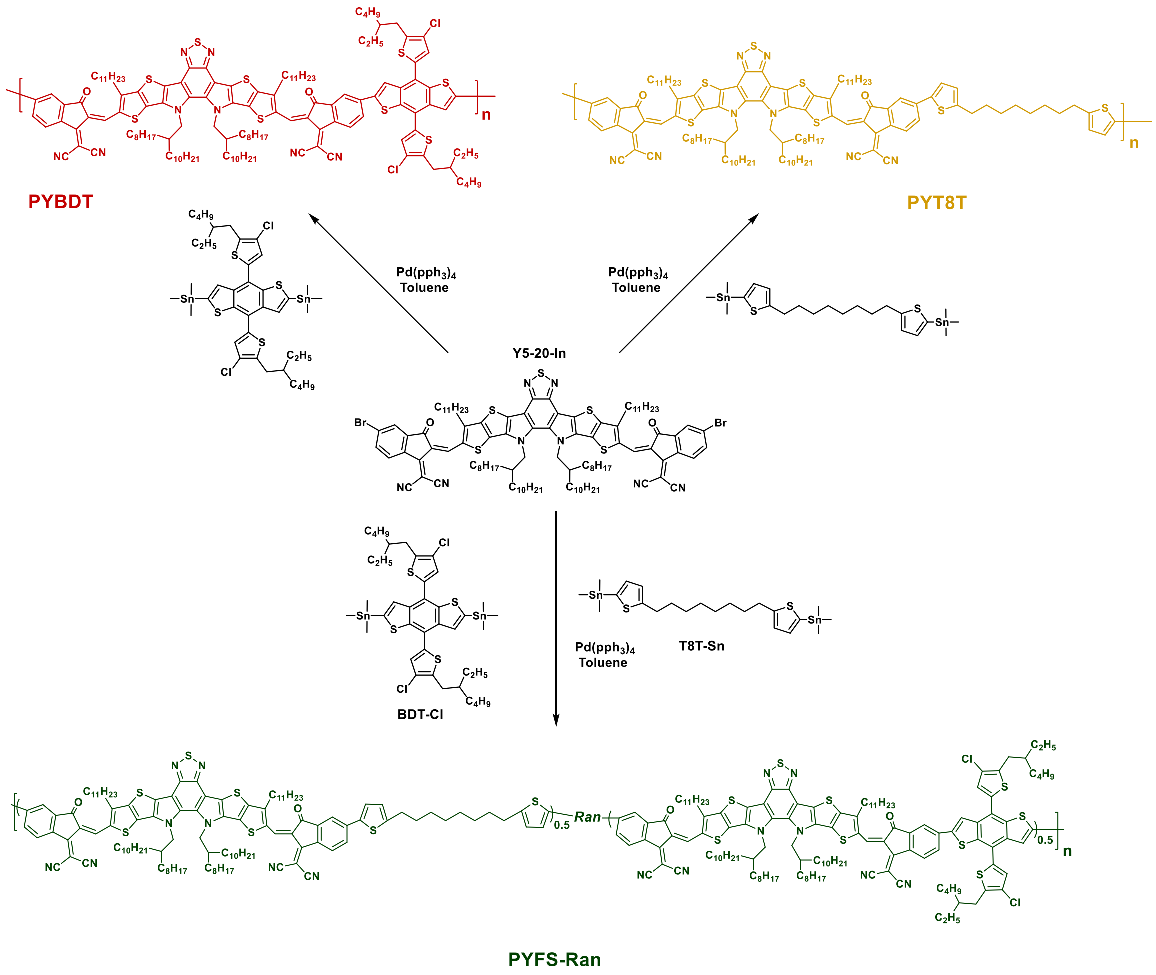

Scheme S2. Synthetic scheme for PYBDT, PYT8T, and PYFS-Ran.

(4) Synthesis of PYBDT

Y5-20-In (140 mg, 0.076 mmol), 4,8-bis(4-chloro-5-(2-ethylhexyl)thiophen-2-yl)-4,8-dihydrobenzo[1,2-b:4,5-b']dithiophene-2,6-diyl)bis(trimethylstannane) (75 mg, 0.076 mmol), and Pd(pph$_3$)$_4$ (4.5 mg, 0.004 mmol) were combined in a 10 mL two-necked flask (**Scheme S2**). Anhydrous toluene (6 mL) was added under the argon atmosphere. The mixture was reacted 24 h at 110 °C. After being cooled down, the reactant mixture was poured into methanol. The precipitate was filtered and Soxhlet extracted with methanol, hexane, and chloroform sequentially. The extracted solution was concentrated and precipitated into 200 mL methanol, filtered and dried under vacuum to give the dark solid. (110 mg, 63%) (M_n= 21 kg mol^{-1}, $Đ$ = 1.8).

^{1}H NMR (300 MHz, CDCl$_3$) δ 9.29–8.66 (broad, 4H), 8.42–7.94 (broad, 4H), 7.83–7.28 (broad, 4H), 5.15–4.57 (m, 4H), 3.52–2.95 (m, 8H), 2.47–2.20 (m, 2H), 2.05–0.66 (m, 148H).

(5) Synthesis of PYT8T

Y5-20-In (200 mg, 0.107 mmol), 1,8-bis(5-(trimethylstannyl)thiophen-2-yl)octane (65 mg, 0.107 mmol) and Pd(pph$_3$)$_4$ (6 mg, 0.0053mmol) were combined in a 10 mL two-necked flask (**Scheme S2**). Anhydrous toluene (6 mL) was added under the argon atmosphere. The mixture was reacted for 24 h at 110 °C. After being cooled down, the reactant mixture was poured into methanol. The precipitate was filtered and Soxhlet extracted with methanol, hexane, and chloroform. The extracted solution was concentrated and precipitated into 200 mL methanol, filtered and dried under vacuum to give the dark solid. (168 mg, 90%); (M_n= 14 kg mol^{-1}, $Đ$ = 1.8). ^{1}H NMR (300 MHz, CDCl$_3$) δ 9.25 – 8.90 (broad, 2H), 8.70 – 8.52 (broad, 2H), 8.12 – 7.66 (broad, 4H), 7.50 – 7.30 (broad, 2H), 6.97 – 6.70 (broad, 2H), 5.25 – 4.35 (m, 4H), 3.36 – 2.68 (m, 8H), 2.31 – 2.07 (m, 2H), 1.95 – 1.62 (m, 8H), 1.62 – 0.55 (m, 122H).

(6) Synthesis of PYFS-Ran

Y5-20-In (200 mg, 0.107 mmol), 4,8-bis(4-chloro-5-(2-ethylhexyl)thiophen-2-yl)-4,8-dihydrobenzo[1,2-b:4,5-b']dithiophene-2,6-diyl)bis(trimethylstannane (52 mg, 0.053 mmol), 1,8-bis(5-(trimethylstannyl)thiophen-2-yl)octane (32.2 mg, 0.053 mmol) and $Pd(pph_3)_4$ (6 mg, 0.0053 mmol) were combined in a 10 mL two-necked flask (**Scheme S2**). Anhydrous toluene (6 mL) was added under the argon atmosphere. The mixture was reacted for 24 h at 110 °C. After being cooled down, the reactant mixture was poured into methanol. The precipitate was filtered and Soxhlet extracted with methanol, hexane, and chloroform sequentially. The extracted solution was concentrated and precipitated into 200 mL methanol, filtered and dried under vacuum to give the dark solid. (165 mg, 80 %), (M_n= 17 kg mol^{-1}, $Đ$ = 2.1).

^{1}H NMR (300 MHz, $CDCl_3$) δ 9.40 – 8.90 (broad, 2H), 8.90 – 8.45 (broad, 2H), 8.33 – 7.68 (broad, 5H), 7.59 – 7.33 (broad, 2H), 7.08 – 6.68 (broad, 1H), 5.30 – 4.33 (broad, 4H), 3.42 – 2.70 (broad, 8H), 2.45 – 2.10 (broad, 2H), 2.10 – 0.41 (broad, 139H).

Characterizations: A UV-1800 spectrophotometer was used for the UV−Vis absorption spectra. The M_n and $Đ$ of the PSMAs were determined by gel permeation chromatography (GPC) measurements with an Agilent GPC 1200 instrument equipped with a refractive index detector, in the condition of *ortho*-dichlorobenzene (*o*-DCB) eluent at 80 °C calibrated with polystyrene standards. The differential scanning calorimetry (DSC) profiles were obtained by TA Instruments DSC 25 with heating and cooling rates of 10 °C min^{-1} from 20 to 350 °C. The melting temperature (T_m) and melting enthalpy (ΔH_m) of the polymers were estimated from the 2nd heating cycles to remove thermal histories of the polymers. The atomic force microscopy (AFM) images were measured by NX10 from Park Systems. M_n and $Đ$ of the PM6 were determined by GPC analyses in 1,2,4-trichlorobenzene at 150 °C. Grazing incidence wide-angle X-ray scattering (GIXS) measurements were conducted at the Pohang Accelerator Laboratory (beamline 9A, Republic of Korea), with incidence angles between 0.12 - 0.14°. Correlation length (L_c) values of the crystallites were calculated using the Scherrer equation:

$$L_\mathrm{c} = \frac{2\pi K}{\Delta_q}$$

(K (shape factor) = 0.9 and Δ_q = full width half maximum (FWHM) of the scatterings)

The resonant soft X-ray scattering (RSoXS) experiment was performed at beamline 11.0.1.2 in the S11 Advanced Light Source (United States). Blend films for the RSoXS measurement were prepared on a 100 nm-thick, 1.0 mm × 1.0 mm Si_3N_4 membrane supported by a 200-μm thick, 5 mm × 5 mm silicon frame (Norcada Inc.). The domain size of a blend film was approximated to be half of the domain spacing (domain spacing= $2\pi q_{\mathrm{peak}}^{-1}$) from the RSoXS profile. The relative domain purity was estimated as the relative ratio of square-root of the integrated scattering intensity in the Iq^2 vs. q plot. The integration range in this study was q = 0.0003 to 0.0100 $Å^{-1}$.

Bruker Avance Drx 300 MHz and 500 MHz FT-NMR spectrometers were used to measure ^{1}H NMR and ^{13}C NMR spectra. The chemical shifts in the spectra have units of ppm. Cyclic voltammetry (CV) was performed using a EG and G Parc model 273 Å potentiostat/galvanostat system in a 0.1 M tetrabutylammonium perchrolate solution with nitrogen degassed anhydrous acetonitrile as the supporting electrolyte, at a scanrate of 50 mV s^{-1}. A glassy carbon electrode was used as the working electrode. A platinum wire was used as the counter electrode, and an Ag/AgCl electrode was used as the reference electrode. The redox couple ferricenium/ferrocene was used as external standard. HOMO and LUMO energy levels were estimated from cyclic voltammetry:

E_{HOMO} (eV) = $-(E_{onset}^{ox.} - E_{onset}^{Fc/Fc+}) + E_{HOMO}^{Fc}$; ELUMO (eV) = $-(E_{onset}^{red.} - E_{onset}^{Fc/Fc+}) + E_{HOMO}^{Fc}$; $E_{onset}^{Fc/Fc+}$= 0.44 eV, E_{HOMO}^{Fc}= −4.8 eV.

Pseudo-freestanding tensile test: The films were prepared with the same condition as that used for the all-PSC fabrications. The films were spin-casted onto polystyrene sulfonic acid-coated glass substrates, and cut into a dog-bone shape by a femtosecond laser. Then, the films were floated onto the water surface, and attached to the grips by van der Waals forces. The strain was applied at a fixed strain rate (0.8×10^{-3} s^{-1}), and the tensile load values were measured by a load cell with high resolution (LTS-10GA, KYOWA, Japan). Elastic modulus was calculated using the least square method for the slope of the linear region of the stress–strain curve within 0.5% strain. The crack-onset strain (COS) of a thin film was determined as the strain value that the tensile load starts to decrease rapidly by cracking.

Fabrication and Characterization of All-Polymer Solar Cells (All-PSCs)**:** The all-PSCs with a normal architecture (indium tin oxide (ITO)/ poly(3,4-ethylenedioxythiophene):poly(styrenesulfonate) (PEDOT:PSS)/active layer/PNDITF3N-Br/Ag) were prepared with the following procedures. ITO-coated glass substrates were treated by ultrasonication with deionized water, acetone, and isopropyl alcohol. Then, the ITO substrates were dried for 6 h in an oven (70 °C) at an ambient pressure, and then plasma treated for 10 min. Spin-coating of the PEDOT:PSS solution (Clevios, AI4083) was performed at 3000 rpm for 30 s onto the ITO substrates. Then, the film/substrate was annealed in the air for 15 min at 150 °C before transferring into an N_2-filled glovebox. The active layer solutions were dissolved together in *ortho*-xylene (*o*-XY) with an optimized condition (donor:acceptor blend weight ratio = 1:1, concentration = 22 mg mL^{-1}, and 1-fluoronaphtalene 3 vol%), and then heated for 2 h at 100 °C. The solution was spin-coated onto the PEDOT:PSS/ITO substrate to form an active layer with the thickness of 100-110 nm. Then, the samples were dried with high vacuum (< 10^{-6} torr) for 30 min and annealed at 120 °C for 10 min. Next, PNDITF3N-Br in methanol (1 mg ml^{-1}) was spin-coated with the condition of 2500 rpm for 30 s. Finally, Ag (120 nm) was deposited under high vacuum (~10^{-6} Torr) in an evaporation chamber. Optical microscopy (OM) was used to measure the exact photoactive area of the mask (0.09 cm^2). Keithley 2400 SMU instrument was used to measure the photovoltaic efficiency of the devices under an Air Mass 1.5 G solar simulator (100 mW cm^{-2}, solar simulator: K201 LAB55, McScience Inc.), satisfying the Class AAA, ASTM Standards. K801SK302 (McScience Inc.) was used as a standard silicon reference cell to calibrate the exact solar intensity. K3100 IQX instrument (McScience Inc.) was used to analyze the external quantum efficiency (EQE) spectra, equipped with a monochromator (Newport) and an optical chopper (MC 2000 Thorlabs).

In situ UV-Vis absorption measurement : The absorption spectra were obtained using a HRR2000+CG spectrometer, equipped with a DH-2000-BAL light source. The OceanView spectroscopy software was applied for the measurements. The pristine and blend solutions were deposited on glass substrates and spin-coated with the same conditions used for the all-PSC fabrication. The UV–Vis absorption spectra of the samples were obtained in a very short time interval of 0.09 s during the spin-coating process (wavelength range: 300–900 nm). The saturation time (t_{sat}) is defined as the point at which the absorbance starts to become constant during the spin-coating process, displaying a quenched morphology in film state.

IS All-PSC Fabrication: Normal-type IS-PSCs with a device configuration (thermoplastic polyurethanes (TPU)/modified PH1000/AI4083/photoactive layers/PNDITF3N-Br/eutectic gallium indium (EGaIn)) were fabricated. The modified PH1000 solution was prepared to contain 5 vol% of dimethyl sulfoxide (DMSO) (to increase the electrical conductivity of PH1000), 2 vol% of polyethylene glycol (PEG) (to improve mechanical stretchability), and 0.5 vol% of Zonyl fluoro surfactant (FS-30) (to enhance the surface wettability). Then the solution was spin-coated at 1200 rpm for 40 s on the plasma-treated TPU substrate and treated for 20 min at 100 °C in air. Next, AI4083 (with FS-30 0.5 vol%) hole transporting layer was spin-coated at 2500 rpm for 40 s on the PH1000/TPU substrate and dried at 100 °C for 20 min. Subsequently, the photoactive layers were spin-coated with the same condition as that used for the all-PSC fabrication on the rigid ITO/glass substrate. Then, the PNDITF3N-Br solution in methanol (1 mg mL^{-1}) was spin-coated at 2000 rpm for 40 s to yield a 5 nm thick electron transporting layer on the active layer. Finally, EGaIn liquid metal was sprayed on the layer through a deposition mask. The photovoltaic performances of IS all-PSCs were tested by the same instruments as those used for the measurement of the performances of the rigid all-PSCs, except for the stretching jig shown in **Fig. 7b**.

Supporting Figures and Tables

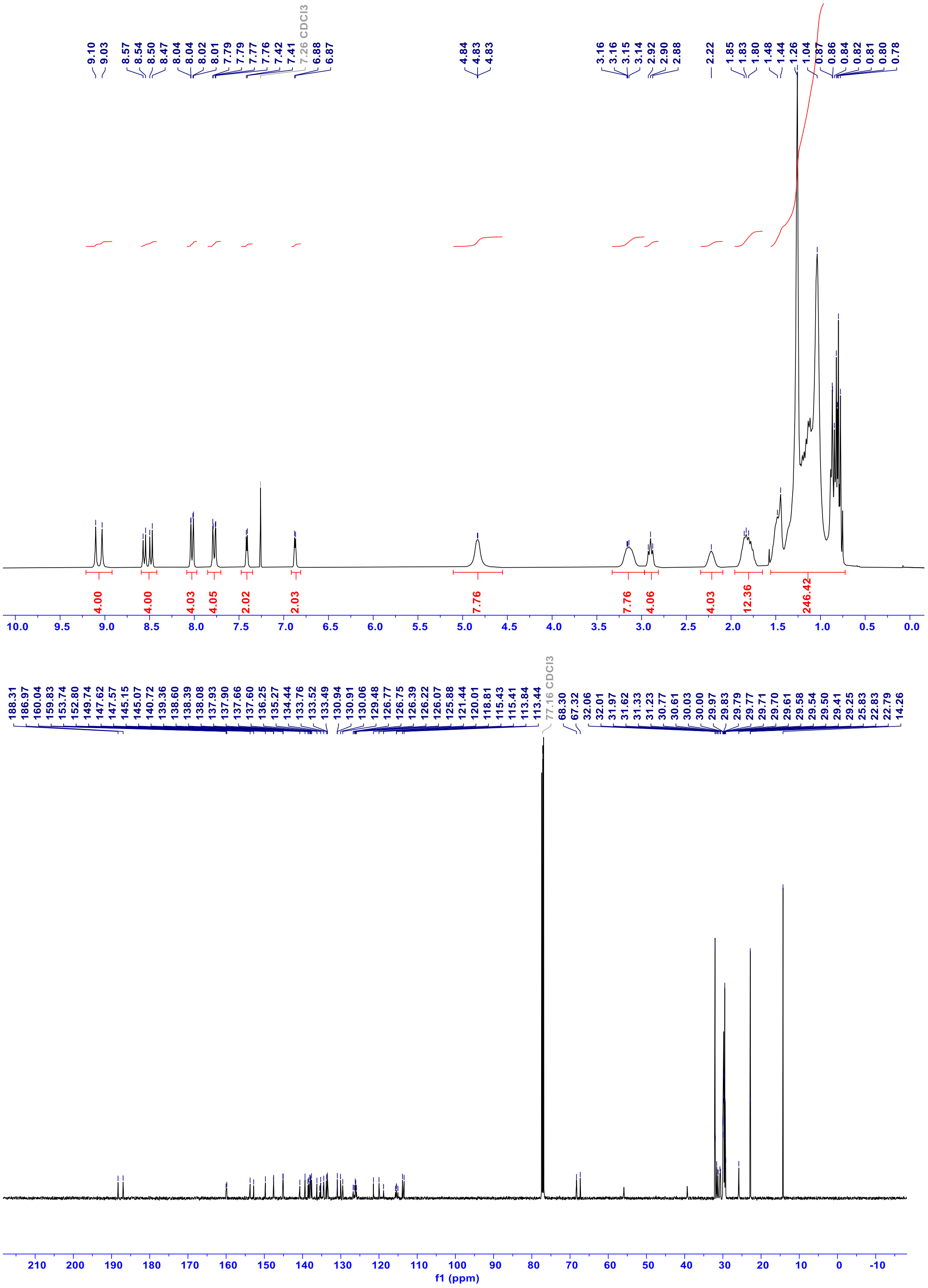

Fig. S1. ^{1}H NMR and ^{13}C NMR spectra of Y5-T8T-Br in $CDCl_3$.

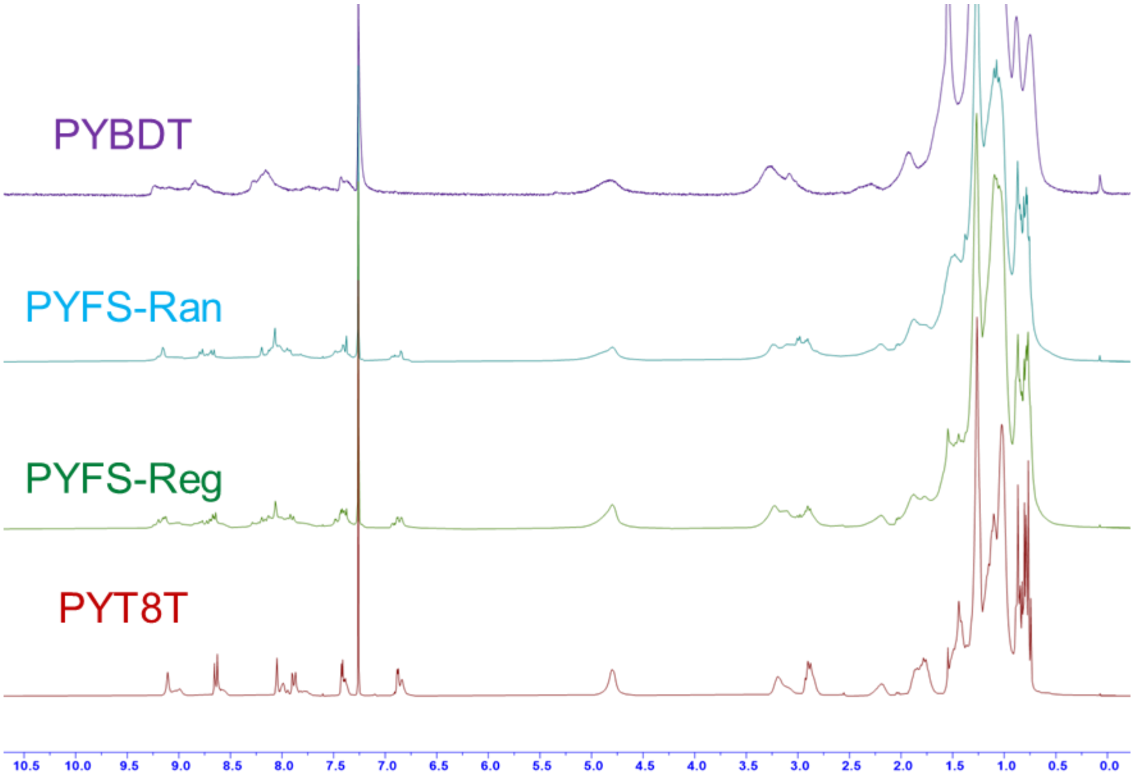

Fig. S2. ^{1}H NMR spectra of PSMAs in $CDCl_3$.

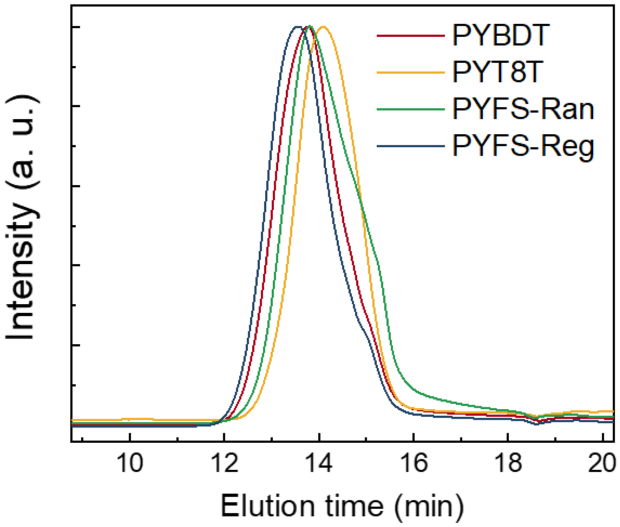

Fig. S3. GPC profiles of the PSMAs.

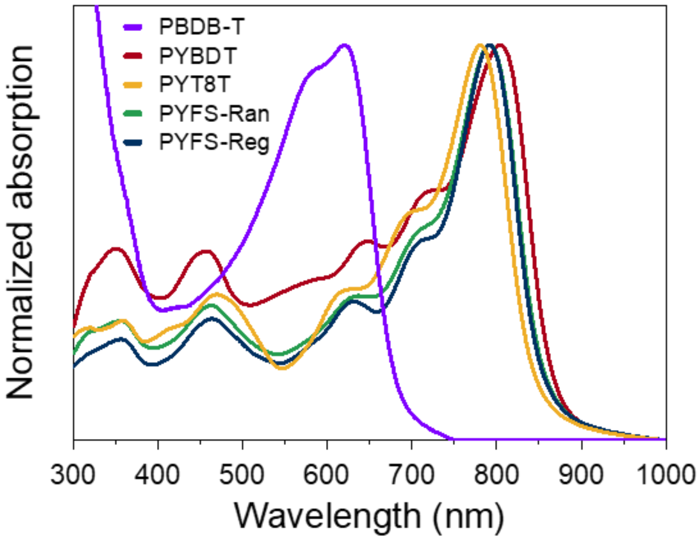

Fig. S4. Normalized film UV-Vis absorption of the P_D and PSMAs.

Table S1. Solubilities of the PSMAs in *o*-XY solvents at 100°C.

PSMA	**Solubility [mg mL^{-1}]**^{a}
PYBDT	10.5
PYT8T	21.3
PYFS-Ran	15.4
PYFS-Reg	13.7

^{a}in *o*-XY solutions at 100 °C (filtered by syringe filters with a pore size of 200 nm in diameter).

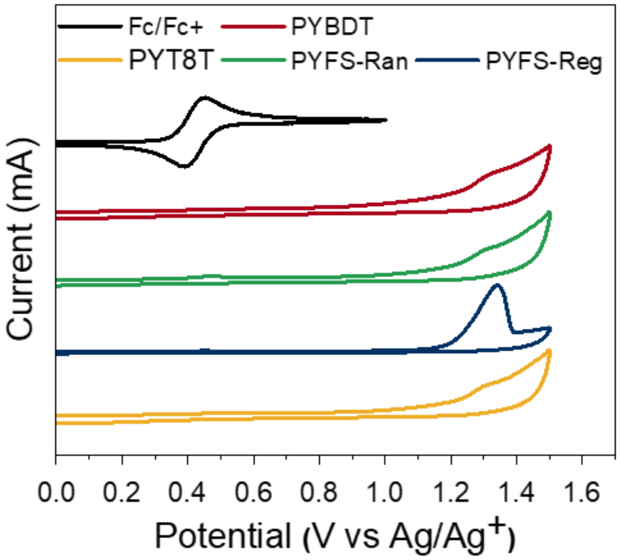

Fig. S5. Cyclic voltamogramms of the PSMAs.

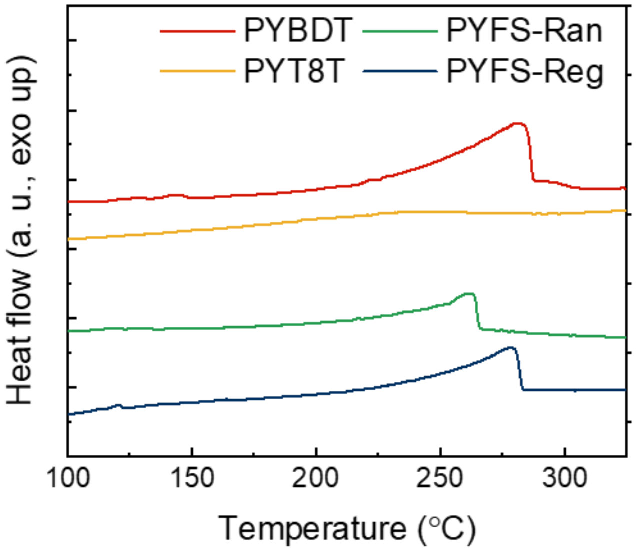

Fig. S6. DSC thermograms of the first cooling cycles of the PSMAs.

Table S2. T_c and ΔH_c values of the PSMAs estimated from the first cooling cycle of DSC measurements.

Polymer	T_c **(°C)**	ΔH_c **(J g^{-1})**
PYBDT	281	21.2
PYT8T	–	–
PYFS-Ran	262	12.4
PYFS-Reg	278	15.5

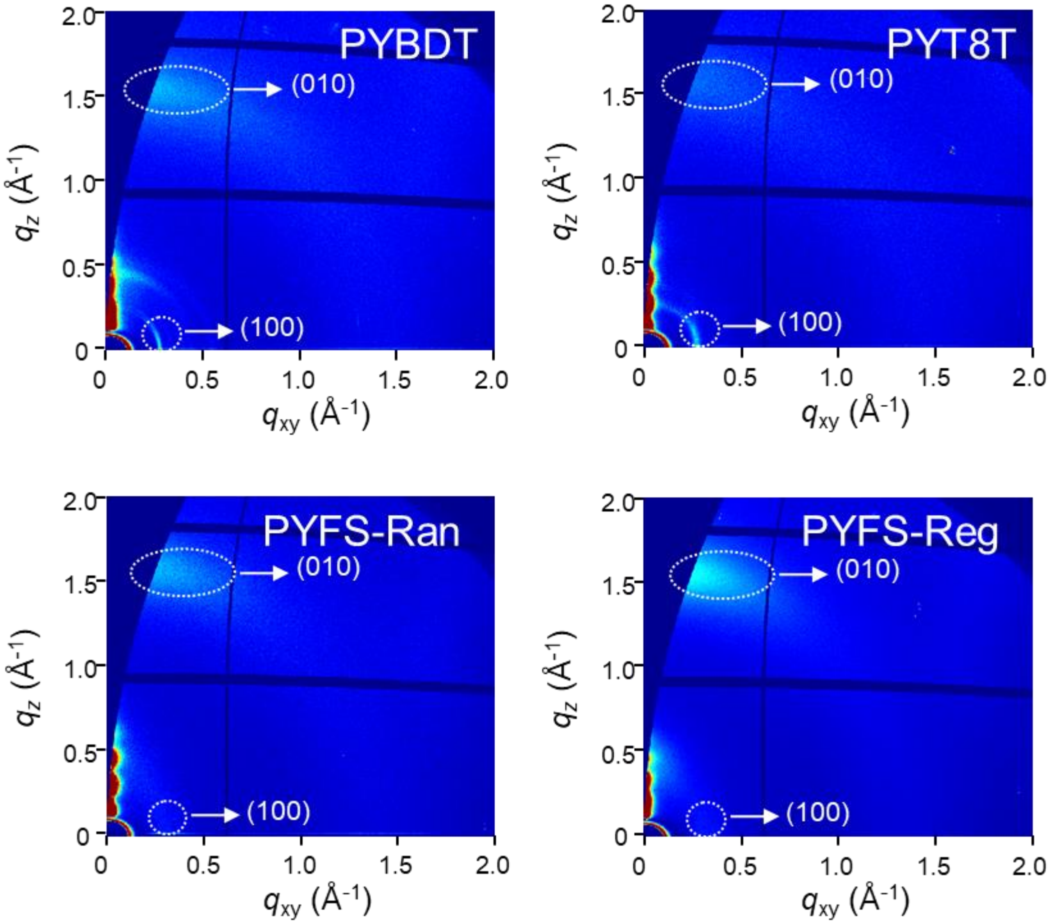

Fig. S7. GIXS 2D-images of the pristine PSMAs.

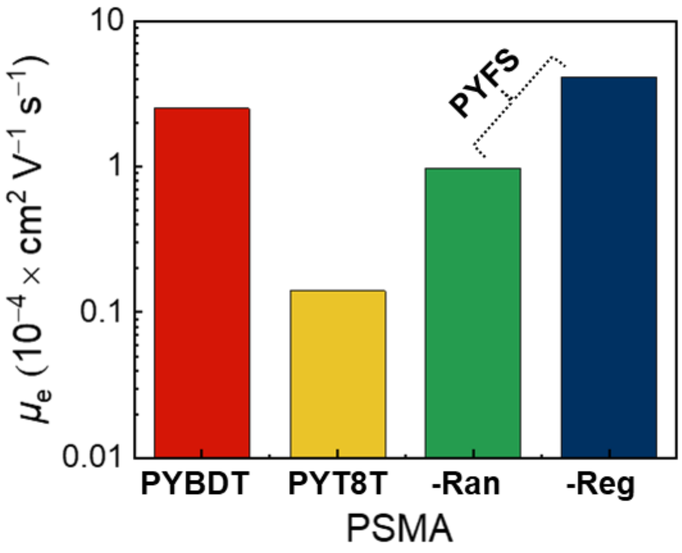

Fig. S8. SCLC μ_e plots of the pristine PSMAs.

Table S3. SCLC mobilities of the pristine PSMAs.

PSMA	**μ_e (cm^2 V^{-1} s^{-1})**
PYBDT	2.5×10^{-4}
PYT8T	1.4×10^{-5}
PYFS-Ran	9.8×10^{-5}
PYFS-Reg	4.1×10^{-4}

Table S4. PCE_{max} values of the all-PSCs achieved with non-halogenated solvent processing in other works and this work.

Blend	**Solvent**	**PCE_{max} (%)**	**Year**	**Reference**
PBDB-T:PYFS-Reg	**o-Xylene**	**16.09**	**2022**	**This work**
PM6:PY-IT	Toluene	16.10	2021	[8]
PM6:L14	o-Xylene	15.62	2021	[9]
PM6:PY-IT	Toluene	15.51	2021	[10]
PBDB-T:PJ1	o-Xylene	14.34	2021	[11]
PM6-PY2F-T	o-Xylene	14.03	2021	[12]
PtzBI-oF:PS1	2-Methyl tetrahdrofuran	13.8	2021	[13]
Nap-SiBTz:N2200	Toluene	11.66	2021	[14]
PtzBI-Si: N2200	2-Methyl tetrahydrofuran	11.76	2019	[15]
PtzBI-Si:N2200	Cyclopentyl methyl ether	11.0	2019	[16]
PtzBI-Si:P(NDI2OD-T2)	2-Methyl tetrahydrofuran	10.1	2017	[17]

Table S5. SCLC mobilities, *P*(E,T), and *P*(C,T) values for PBDB-T:PSMA all-PSCs.

PSMA	μ_h **(cm^2 V^{-1} s^{-1})**	μ_e **(cm^2 V^{-1} s^{-1})**	μ_h/μ_e	***P*(E,T) (%)**[a]	***P*(C,T) (%)**[b]
PYBDT	3.7×10^{-4}	2.0×10^{-4}	1.85	76	73
PYT8T	6.8×10^{-5}	8.6×10^{-6}	7.91	67	62
PYFS-Ran	2.1×10^{-4}	5.4×10^{-5}	3.89	87	83
PYFS-Reg	3.4×10^{-4}	3.7×10^{-4}	0.92	91	88

[a] Exciton dissociation probability ($P(E,T) = J_{sc}/J_{sat}$); [b] Charge collection efficiency ($P(C,T) = J_{\text{maximum power point}}/J_{sat}$).

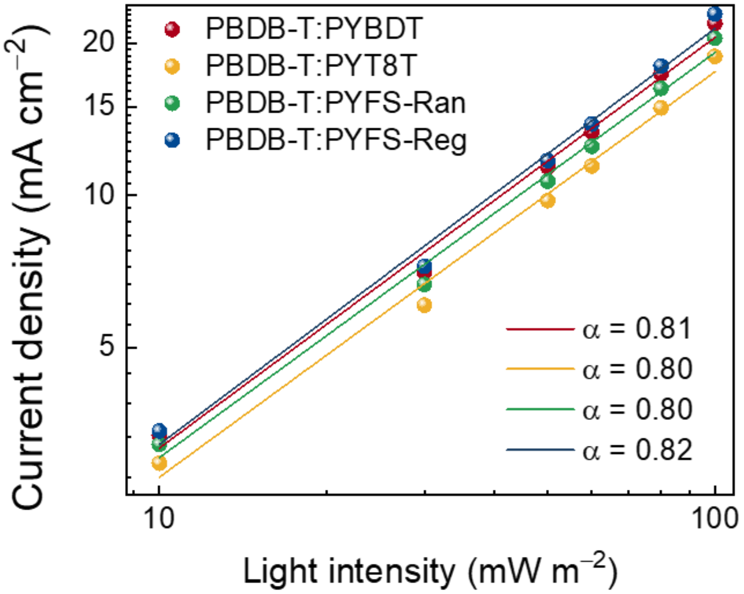

Fig. S9. Light intensity-dependent J_{sc} plots of the all-PSCs.

Table S6. Summary of PCE and COS values of all-PSCs. COS was measured by pseudo free-standing tensile tests.

Blend	Solvent	PCE_{max} (%)	COS (%)	Reference
PBDTTTPD:P(NDI2HD-T)	Chloroform (CF)	6.64	7.2	[18]
PTB7-Th:P-15K	CF	3.12	6.0	[19]
PTB7-Th:P-20K	CF	3.43	11.2	[19]
PTB7-Th:P-48K	CF	4.24	14.4	[19]
PTB7-Th:P(NDI2HD-T)	Chlorobenzene (CB)	5.91	11.6	[20]
PTzBI:N2200	Methyl-tetrahydrofuran (Me-THF)	8.36	15.6	[21]
PTzBI:N2200	CF	4.49	8.1	[21]
PTzBI:N2200	CB	2.92	6.3	[21]
J52:N2200	CF	5.30	19	[22]
PBZ-$2Si_L$:N2200	CF	4.51	15.5	[22]
PBZ-$2Si_M$:N2200	CF	6.89	38.1	[22]
PBZ-$2Si_H$:N2200	CF	6.28	50.2	[22]
PM6:PF2-DTC	CF	8.31	11.3	[23]
PM6:PF2-DTSi	CF	10.77	8.6	[23]
PM6:PF2-DTGe	CF	8.09	6.7	[23]
PBDB-T:P(BDT2BOY5-H)	*ortho*-dichlorobenzene (*o*-DCB)	8.81	19.3	[1]
PBDB-T:P(BDT2BOY5-F)	*o*-DCB	9.83	16.7	[1]
PBDB-T:P(BDT2BOY5-Cl)	*o*-DCB	11.12	15.9	[1]
PBDB-T:PY-O	CF	9.80	9.57	[24]
PBDB-T:PY-S	CF	14.16	8.70	[24]
PBDB-T:PYTS-0.0	CB	13.01	18.84	[25]
PBDB-T:PYTS-0.1	CB	14.19	20.56	[25]
PBDB-T:PYTS-0.3	CB	14.68	21.64	[25]
PBDB-T:PYTS-0.5	CB	7.91	12.39	[25]
PBDB-T:PYTS-1.0	CB	1.71	8.09	[25]
PBDB-T:PY-T (BHJ)	CF	14.06	8.5	[26]
PBDB-T:PY-T (LBL)	CF	15.17	10.5	[26]
PBDB-T:PYFS-Reg	***o*-XY**	**16.09**	**22.4**	**This work**

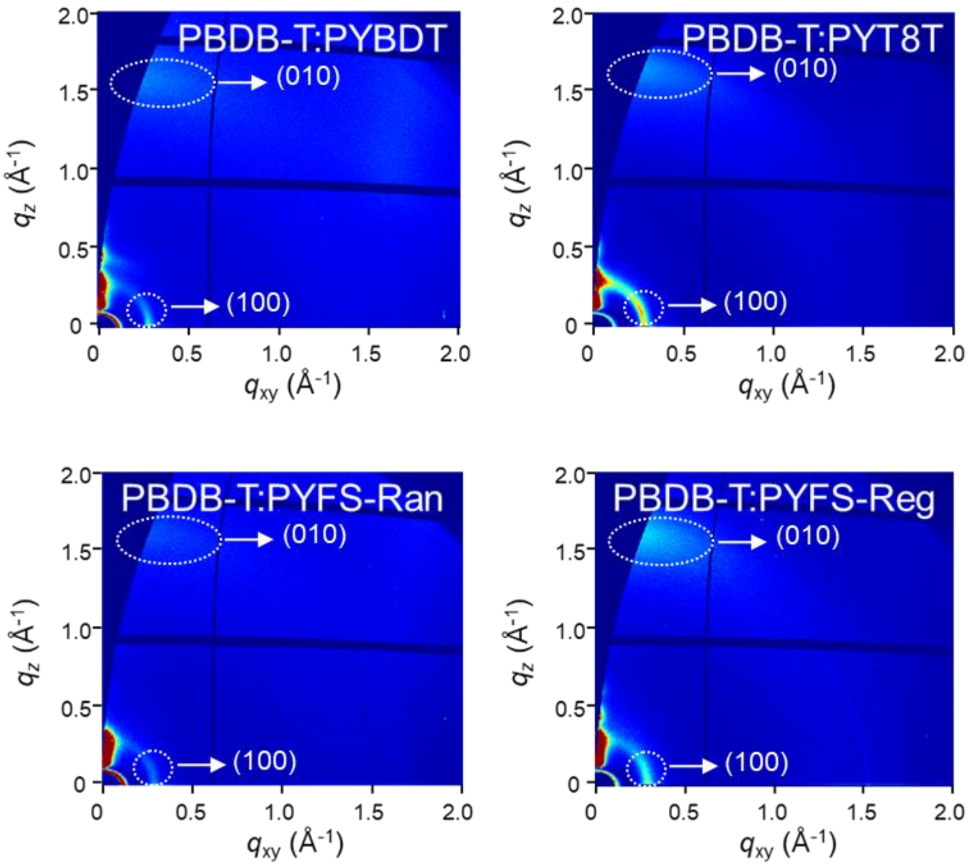

Fig. S10. GIXS 2D-images of the PBDB-T:PSMA blends.

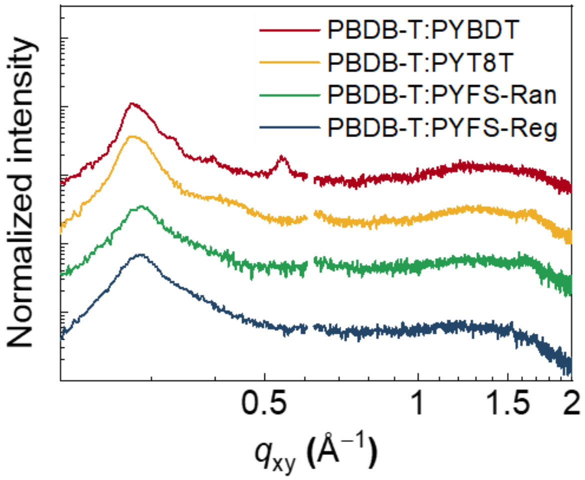

Fig. S11. GIXS linecut profiles in the IP direction of the PBDB-T:PSMA blends.

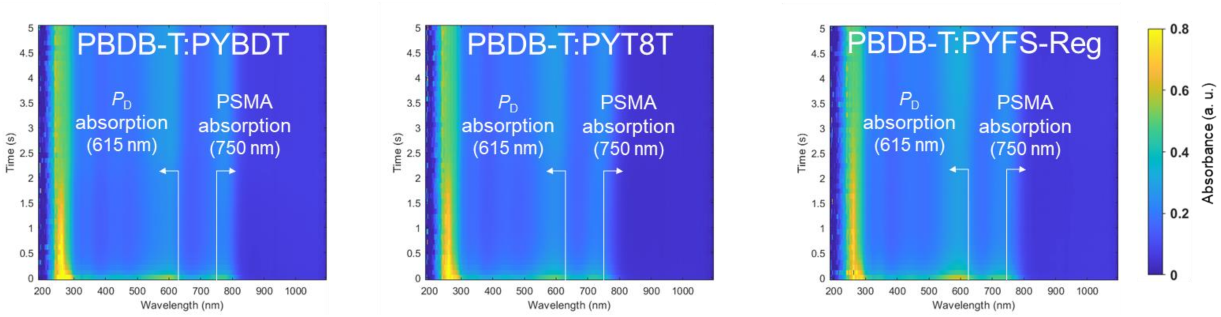

Fig. S12. 2D-images of *in-situ* UV-Vis absorption spectra of the PBDB-T:PSMA blends.

Table S7. Photovoltaic parameters of IS all-PSCs as a function of strain.

PSMA	**Strain (%)**	**V_{oc} [V]**	**J_{sc} [mA cm^{-2}]**	**FF [%]**	**PCE [%]**	**Normalized PCE**
PYBDT	**0**	0.83	17.92	57.12	8.54	1.00
	10	0.83	18.09	55.49	8.35	0.98
	15	0.83	17.05	53.54	7.57	0.89
	20	0.82	15.05	50.63	6.27	0.73
	25	0.73	12.15	47.78	4.26	0.50
	30	0.69	11.01	44.39	3.39	0.40
	35	0.60	9.01	40.47	2.18	0.26
	40	0.46	7.20	31.19	1.03	0.12
	45	0.42	6.42	29.09	0.78	0.09
PYFS-Reg	**0**	0.88	18.58	62.18	10.12	1.00
	10	0.87	18.17	62.96	9.98	0.99
	15	0.87	17.96	63.06	9.86	0.97
	20	0.87	17.65	63.00	9.67	0.96
	25	0.87	16.74	64.1	9.37	0.93
	30	0.87	16.24	64.22	9.09	0.90
	35	0.86	15.90	63.38	8.71	0.86
	40	0.83	15.52	52.44	6.79	0.67
	45	0.83	14.92	51.97	6.44	0.64
	50	0.49	13.98	28.75	1.97	0.20
PYFS-Ran	**0**	0.86	17.21	55.14	8.17	1.00
	10	0.86	16.83	55.6	8.04	0.98
	15	0.86	16.39	56.2	7.91	0.97
	20	0.86	15.75	56.37	7.62	0.93
	25	0.87	15.40	53.85	7.20	0.88
	30	0.87	15.03	53.98	7.04	0.86
	35	0.83	14.46	47.29	5.71	0.70
	40	0.80	12.84	44.42	4.58	0.56
	45	0.35	9.73	26.00	0.88	0.11

References

1. J.-W. Lee, C. Sun, B. S. Ma, H. J. Kim, C. Wang, J. M. Ryu, C. Lim, T. S. Kim, Y. H. Kim, S. K. Kwon and B. J. Kim, *Adv. Energy Mater.*, 2021, **11**, 2003367.
2. Z. H. Luo, T. Liu, R. J. Ma, Y. Q. Xiao, L. L. Zhan, G. Y. Zhang, H. L. Sun, F. Ni, G. D. Chai, J. W. Wang, C. Zhong, Y. Zou, X. G. Guo, X. H. Lu, H. Z. Chen, H. Yan and C. L. Yang, *Adv. Mater.*, 2020, **32**, 2005942.
3. T. Jia, J. B. Zhang, W. K. Zhong, Y. Y. Liang, K. Zhang, S. Dong, L. Ying, F. Liu, X. H. Wang, F. Huang and Y. Cao, *Nano Energy*, 2020, **72**, 104718.
4. X. K. Zhao, Y. Zhao, Q. Ge, K. Butrouna, Y. Diao, K. R. Graham and J. G. Mei, *Macromolecules*, 2016, **49**, 2601-2608.
5. C. Sun, J.-W. Lee, S. Seo, S. Lee, C. Wang, H. Li, Z. P. Tan, S. K. Kwon, B. J. Kim and Y. H. Kim, *Adv. Energy Mater.*, 2022, **12**, 2103239.
6. J. Yao, B. B. Qiu, Z. G. Zhang, L. W. Xue, R. Wang, C. F. Zhang, S. S. Chen, Q. J. Zhou, C. K. Sun, C. Yang, M. Xiao, L. Meng and Y. F. Li, *Nat. Commun.*, 2020, **11**, 2726.
7. Z. H. Wu, C. Sun, S. Dong, X. F. Jiang, S. P. Wu, H. B. Wu, H. L. Yip, F. Huang and Y. Cao, *J. Am. Chem. Soc.*, 2016, **138**, 2004-2013.
8. S. Y. Ding, R. J. Ma, T. Yang, G. Y. Zhang, J. L. Yin, Z. H. Luo, K. Chen, Z. C. Miao, T. Liu, H. Yan and D. F. Xue, *ACS Appl. Mater. Interfaces*, 2021, **13**, 51078-51085.
9. B. Liu, H. Sun, J.-W. Lee, J. Yang, J. Wang, Y. Li, B. Li, M. Xu, Q. Liao, W. Zhang, D. Han, L. Niu, H. Meng, B. J. Kim and X. Guo, *Energy Environ. Sci.*, 2021, **14**, 4499-4507.
10. L. Jin, R. Ma, H. Liu, W. Xu, Z. Luo, T. Liu, W. Su, Y. Li, R. Lu, X. Lu, H. Yan, B. Z. Tang and T. Yang, *ACS Appl. Mater. Interfaces*, 2021, **13**, 34301-34307.
11. J. Zhang, T. Jia, C.-H. Tan, K. Zhang, M. Ren, S. Dong, Q. Xu, F. Huang and Y. Cao, *Sol RRL*, 2021, **5**, 2100076.
12. H. Yu, S. Luo, R. Sun, I. Angunawela, Z. Qi, Z. Peng, W. Zhou, H. Han, R. Wei, M. Pan, A. M. H. Cheung, D. Zhao, J. Zhang, H. Ade, J. Min and H. Yan, *Adv. Funct. Mater.*, 2021, **31**, 2100791.
13. C. Zhu, Z. Li, W. Zhong, F. Peng, Z. Zeng, L. Ying, F. Huang and Y. Cao, *Chem. Commun.*, 2021, **57**, 935-938.
14. T. Gokulnath, J. Choi, H. Jin, H.-Y. Park, K. Sung, Y. Do, H. Park, S. S. Reddy, J. Kim, M. Song, J. Yoon and S.-H. Jin, *ACS Appl. Mater. Interfaces*, 2021, **13**, 28231-28241.
15. L. Zhu, W. Zhong, C. Qiu, B. Lyu, Z. Zhou, M. Zhang, J. Song, J. Xu, J. Wang, J. Ali, W. Feng, Z. Shi, X. Gu, L. Ying, Y. Zhang and F. Liu, *Adv. Mater.*, 2019, **31**, 1902899.
16. Z. Y. Li, L. Ying, P. Zhu, W. K. Zhong, N. Li, F. Liu, F. Huang and Y. Cao, *Energy Environ. Sci.*, 2019, **12**, 157-163.
17. B. Fan, L. Ying, P. Zhu, F. Pan, F. Liu, J. Chen, F. Huang and Y. Cao, *Adv. Mater.*, 2017, **29**, 1703906.
18. T. Kim, J. H. Kim, T. E. Kang, C. Lee, H. Kang, M. Shin, C. Wang, B. W. Ma, U. Jeong, T. S. Kim and B. J. Kim, *Nat. Commun.*, 2015, **6**, 8547.
19. J. Choi, W. Kim, S. Kim, T. S. Kim and B. J. Kim, *Chem. Mater.*, 2019, **31**, 9057-9069.

20. W. Lee, J. H. Kim, T. Kim, S. Kim, C. Lee, J. S. Kim, H. Ahn, T. S. Kim and B. J. Kim, *J. Mater. Chem. A*, 2018, **6**, 4494-4503.
21. B. J. Lin, L. Zhang, H. Zhao, X. B. Xu, K. Zhou, S. Zhang, L. Gou, B. B. Fan, L. Zhang, H. P. Yan, X. D. Gu, L. Ying, F. Huang, Y. Cao and W. Ma, *Nano Energy*, 2019, **59**, 277-284.
22. M. Xu, D. Zhang, Z. Wang, Z. Liu, X. Gao, J. He, Y. Gao, Z. Li and M. Shao, *Chem. Eng. J.*, 2022, **440**, 135829.
23. Q. P. Fan, W. Y. Su, S. S. Chen, W. Kim, X. B. Chen, B. Lee, T. Liu, U. A. Mendez-Romero, R. J. Ma, T. Yang, W. L. Zhuang, Y. Li, Y. W. Li, T. S. Kim, L. T. Hou, C. Yang, H. Yan, D. H. Yu and E. G. Wang, *Joule*, 2020, **4**, 658-672.
24. Q. Wu, W. Wang, Y. Wu, R. Sun, J. Guo, M. M. Shi and J. Min, *Natl. Sci. Rev.*, 2022, **9**, nwab151.
25. Z. Genene, J. W. Lee, S. W. Lee, Q. Chen, Z. Tan, B. A. Abdulahi, D. Yu, T. S. Kim, B. J. Kim and E. Wang, *Adv. Mater.*, 2022, **34**, 2107361.
26. Q. Wu, W. Wang, Y. Wu, Z. Chen, J. Guo, R. Sun, J. Guo, Y. Yang and J. Min, *Adv. Funct. Mater.*, 2021, **31**, 2010411.